remote sensing

MDPI

Article

Identification and Evaluation of the Polycentric Urban Structure: An Empirical Analysis Based on Multi-Source Big Data Fusion

Yuquan Zhou [1,†], Xiong He [2,†] and Yiting Zhu [3,*]

[1] Department of Urban Planning and Spatial Analysis, Sol Price School of Public Policy, University of Southern California, Los Angeles, CA 90089, USA; yuquanzh@usc.edu
[2] School of Geography and Planning, Sun Yat-sen University, Guangzhou 510275, China; hexiong6@mail2.sysu.edu.cn
[3] Key Laboratory of Sustainable Development of Xinjiang's Historical and Cultural Tourism, College of Tourism, Xinjiang University, Urumqi 830046, China
* Correspondence: yiting@xju.edu.cn
† These authors contributed equally to this work.

Abstract: Identifying and evaluating polycentric urban spatial structure is essential for understanding and optimizing current urban development. In order to accurately identify the urban centers of the Guangdong–Hong Kong–Macao Greater Bay Area (GBA), this study firstly fused nighttime light data, POI data, and population migration data based on wavelet transform, then identified the polycentric spatial structure of the GBA by carrying out cluster and outlier analysis, and evaluated the level of different urban centers byconducting geographical weighted regression analysis. Using data fusion, we identified 4579.81 km^2 of the urban poly-center area in the GBA, with an identification accuracy of 93.22%. Although the number and spatial extent of the identified urban poly-centers are consistent with the GBA development plan outline, the poly-center level evaluation results are inconsistent with the development plan, which shows there are great differences in actual development levels among different cities in the GBA. By identifying and grading the polycentric spatial structure of the GBA, this study accurately analyzed the current spatial distribution and could provide policy implications for the GBA's future development and planning.

Keywords: urban agglomeration; big data; nighttime light data; data fusion; spatial planning

Citation: Zhou, Y.; He, X.; Zhu, Y. Identification and Evaluation of the Polycentric Urban Structure: An Empirical Analysis Based on Multi-Source Big Data Fusion. *Remote Sens.* **2022**, *14*, 2705. https://doi.org/10.3390/rs14112705

Academic Editor: Danlin Yu

Received: 3 May 2022
Accepted: 2 June 2022
Published: 4 June 2022

1. Introduction

Urban agglomerations, as the main spaces for a region or country's high-quality economic development activities, play a vital role in regional and national economic growth [1,2]. In January 2019, the "Report on Influence of the Four Great Bay Areas (2018): New York, San Francisco, Tokyo, Guangdong–Hong Kong–Macau Greater Bay Area" released by the Chinese Academy of Social Sciences, pointed out that the economic impact of the Guangdong–Hong Kong–Macao Greater Bay Area (GBA) ranks first among the four major bay areas in the world [3]. Additionally, with its polycentric advantage, the GBA has the potential to become the world's foremost bay area [3].

With rapid urban development, the form and function of the urban spatial structure have undergone substantial changes. Some metropolitan areas have gradually evolved from an initial monocentric urban spatial structure to a polycentric urban spatial structure [4,5]. Based on planning and development experience, the polycentric spatial structure is ideal for a mature urban agglomeration [6]. The polycentric urban spatial structure generally includes several main centers and subcenters. The main center is often the most densely populated area of the city, including the central business district (CBD), which is the core of the city [7,8]. The subcenter, including satellite cities and new airport cities, is the area that has a certain distance from the main center and has significantly different and relatively more intensive urban activities compared to the surrounding areas. The

primary function of subcenters lies in evacuating the over-concentrated population and economic activities in the main center [9]. Urban agglomerations, including the GBA, generally adopt a poly-center spatial structure development model in development plans [10]. However, effectively identifying and evaluating the polycentric spatial structure of urban agglomerations remains a difficult problem for scientific planning implementation [4,11].

The existing polycentric urban agglomeration spatial structure research used different data sources and analysis methods. One of the earliest data used for urban center identification are demographic and socioeconomic data [12]. For example, researchers used economic data to identify areas with high GDP as urban centers [13], and census data to identify macro-scale urban centers [14]. In 2003, researchers developed a relatively complex but more accurate method for identifying urban centers based on demographic data [15]. Using locally weighted regression and spatial autocorrelation analysis, the above method defines an urban subcenter as a densely populated place that has a certain distance from the primary urban center. This method is widely accepted by the academic community and significantly impacts the study of polycentric urban structures [16,17]. Subsequent studies continued to contribute to polycentric urban structure studies by using analysis techniques such as local autocorrelation and geographically weighted regression (GWR) to identify urban centers [18,19]. However, identifying urban centers based on demographic and socioeconomic data requires a basic understanding of the study area and has a certain degree of subjectivity [20]. Compared with statistical data, remote sensing images can reflect the objective spatial characteristics of the urban landscape and infrastructure and, therefore, are widely used in the study of urban space [21]. The nighttime light data, as the most commonly used remote sensing data in this context, reflect the spatial characteristics of the city using the degree of urban brightness at night [22]. The key to using nighttime lights to identify urban spatial structures is to determine their extraction threshold. Researchers proposed a natural city method to identify the city center [23], which determines the extent of the urban center using the difference between the upper and lower end of the pixel value and the mean pixel value of the nighttime light data [24]. Although nighttime light data have higher spatial stability and objectivity than statistical data, they suffer from the shortcoming of light spillover effects and cannot reflect the actual activity of people in urban space [25,26].

In recent years, the application of urban big data has played a critical role in urban geography and planning, providing a dynamic approach for the observation of urban spatial characteristics [27]. For example, researchers can use Point of Interest (POI) data for detailed analysis of different urban functional areas [28], mobile phone signaling data for the urban jobs and housing space and commuting analysis [29], and population movement data to reflect the element flows and interactions between and within cities [30]. However, big data usage in urban spatial analysis is more inclined towards cartographic simulation; thus, urban spatial structure analysis still lacks objective and scientific methods [31]. Therefore, researchers have begun to shift their research focus toward fusing multi-source big data and traditional data to improve the accuracy of urban spatial research [32,33]. Existing studies have shown that multi-source big data fusion has achieved good results in urban built-up area extraction [34], urban boundary delineation [35], and urban center identification [36], significantly improving the observation accuracy of urban spatial structure [37].

At present, studies related to the application of data fusion mainly use image signaling methods such as wavelet transform to fuse NTL data and POI data, which means carrying out pixel-level image fusion, so that the fused image retains the basic features and information of the original image to the maximum extent [38,39]. In 2021, He and others successfully delineated the boundaries of urban agglomerations and extracted urban built-up areas by using this method to fuse NTL data, POI data, and population migration data. However, the fused data still has a certain amount of noise and some features are too different to be fused [31,40]. Therefore, it is not only necessary to fuse the data, but also necessary to denoise and optimize the fused data through feasible methods. On the basis of previous studies, wavelet transform is firstly used to fuse NTL data, POI data,

and population migration data, then spectral difference segmentation is used to optimize the fused data, then case analysis is carried out to identify and evaluate the less involved polycentric areas of urban agglomeration, which is of high theoretical and practical value.

As one of the largest urban agglomerations in China, the Guangdong–Hong Kong–Macao Greater Bay Area (GBA) has remarkable urban development and economic growth. To accurately identify and evaluate the GBA's spatial structure, this study fuses nighttime light data, POI data, and population migration data to identify and evaluate the polycentric spatial structure of the GBA urban agglomeration. This work extends the previous studies by fusing multi-source big data and further proposing a polycentric hierarchical evaluation method based on the identification results of urban centers. [41,42]. The study results of identified and evaluated GBA urban centers can be used to assess urban agglomerations' development status accurately so as to provide a theoretical reference for the urban planning strategies for urban agglomerations.

2. Materials and Methods

2.1. Study Area

The Guangdong–Hong Kong–Macao Greater Bay Area (hereinafter referred to as the GBA) consists of the Special Administrative Regions of Hong Kong and Macau and nine cities in Guangdong Province, namely Guangzhou, Shenzhen, Zhuhai, Foshan, Huizhou, Dongguan, Zhongshan, Jiangmen, and Zhaoqing. The city composition (Figure 1) has a total area of 56,000 square kilometers. According to the seventh national census of 2020, the population of the GBA has reached 83.0598 million, making it the largest urban agglomeration in China. Due to historical reasons, the Greater Bay Area has formed a unique management pattern of "one country, two systems" (on the premise of adhering to the One-China principle, the main body of the country will adhere to the socialist system, and Hong Kong, Macao, and Taiwan will maintain their original capitalist system). Political, legal and administrative differences make the GBA unique among urban agglomerations worldwide.

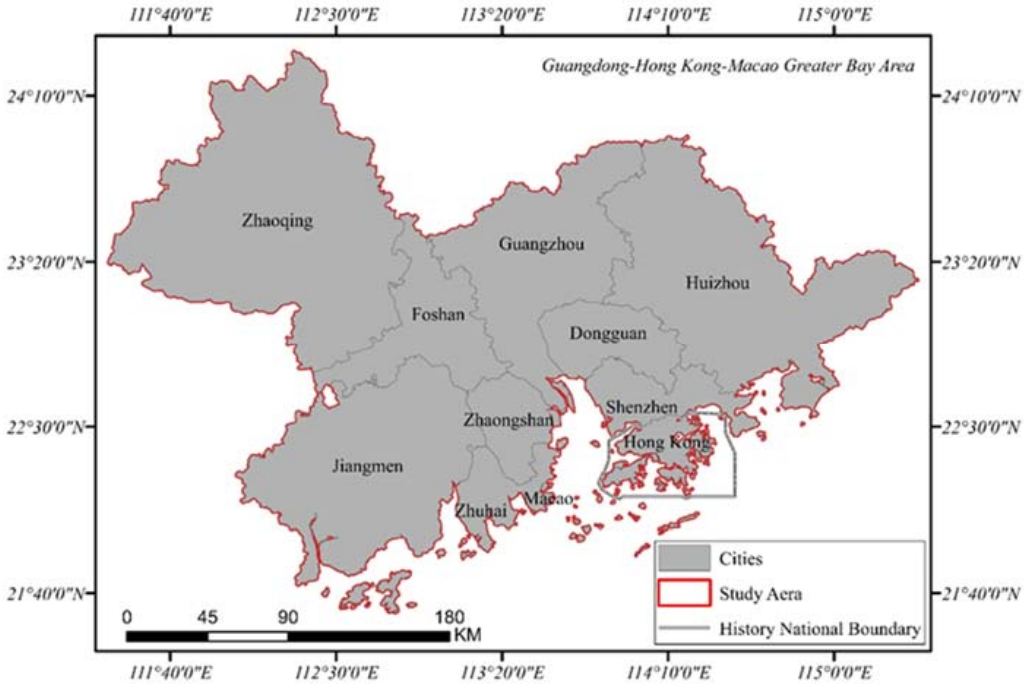

Figure 1. The Guangdong–Hong Kong–Macao Greater Bay Area (GBA).

2.2. Study Data

The data used in this study include nighttime light data, POI data, and population migration data. The nighttime light data is Luojia-01 data, which is provided by the Luojia-

01 experimental satellite launched by Wuhan University in 2018. The wavelength range of the data is 480–800 μm, with a resolution of 130 m and a width of 260 km. By constructing the on-orbit geometric radiometric calibration model for daytime imaging calibration and nighttime imaging correction, Luojia-01 data has realized the noctilucent imaging with high sensitivity, high dynamic range, and high geometric radiation quality, reaching the leading level of similar satellite sensors in the world. Additionally, Luojia-01 data has also proposed a weakly rendezvous plane-area net adjustment method, which makes its absolute geometric accuracy superior to other nighttime light data. We accessed the nighttime light data in the GBA from October 2018 to March 2019 from the Hubei Data and Application Network of the High-resolution Earth Observation System (http://59.175.109.173:8888/, accessed on 21 March 2021). After radiation correction, radiation brightness conversion, and multi-period average processing, the nighttime light data of the GBA are shown in Figure 2.

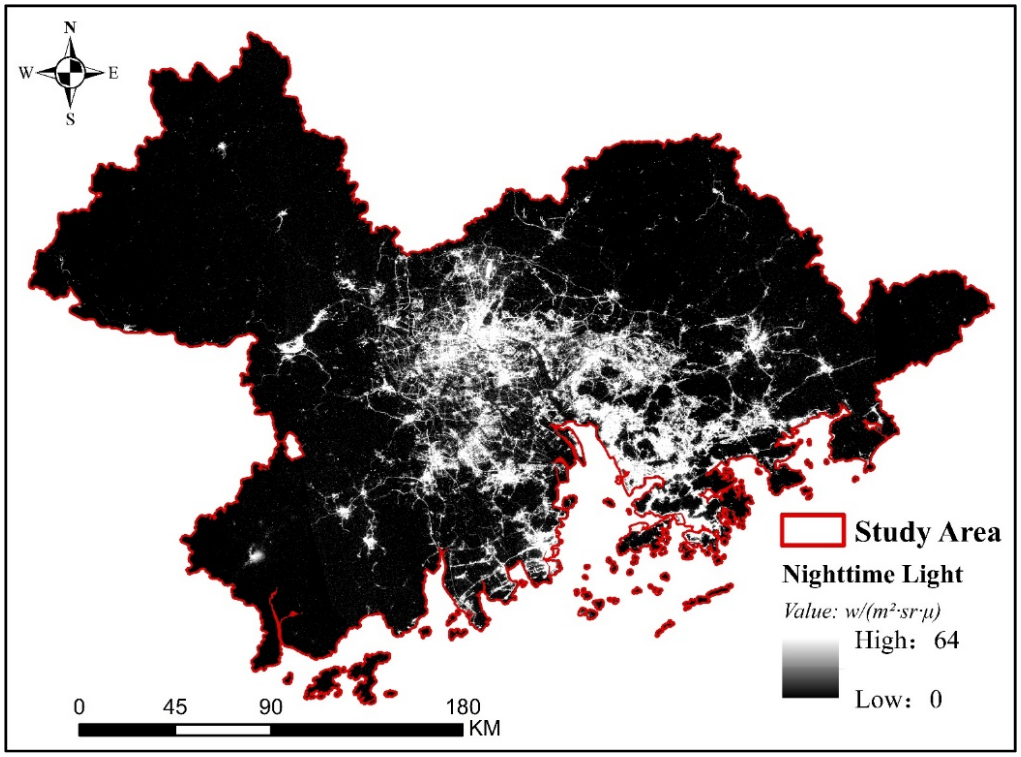

Figure 2. Preprocessing result of nighttime light data in the GBA.

As a map provider of digital content, navigation, and location service solutions, Amap's POI solution provides users great convenience in navigation and regional search, enabling it to occupy most of the electronic map market in China. POI data used in this study were obtained via Amap API in 2021, including POI attributes for name, address, coordinates, and category. After checking, screening, and filtering POI data, the total number of POIs in the GBA is 2477184 (Figure 3).

The population migration data were obtained by accessing the Tencent location big data platform and randomly selecting 12 weeks of population migration data in the GBA from 1 January to 31 December 2020. Data attributes include origin and destination point, longitude and latitude, population inflow, population outflow, and the migration ratio of different modes of transportation. Finally, we uniformly resampled the data to a spatial resolution of 130 m (Figure 4). The details of the accessed data are listed in Table 1.

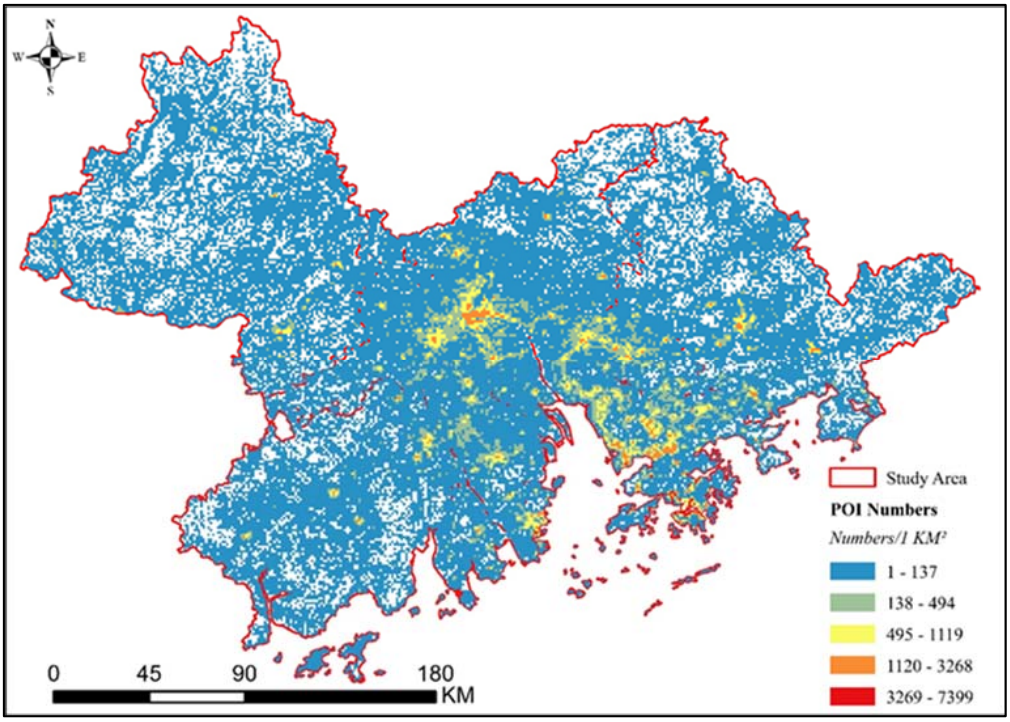

Figure 3. Spatial distribution of POI data in the GBA.

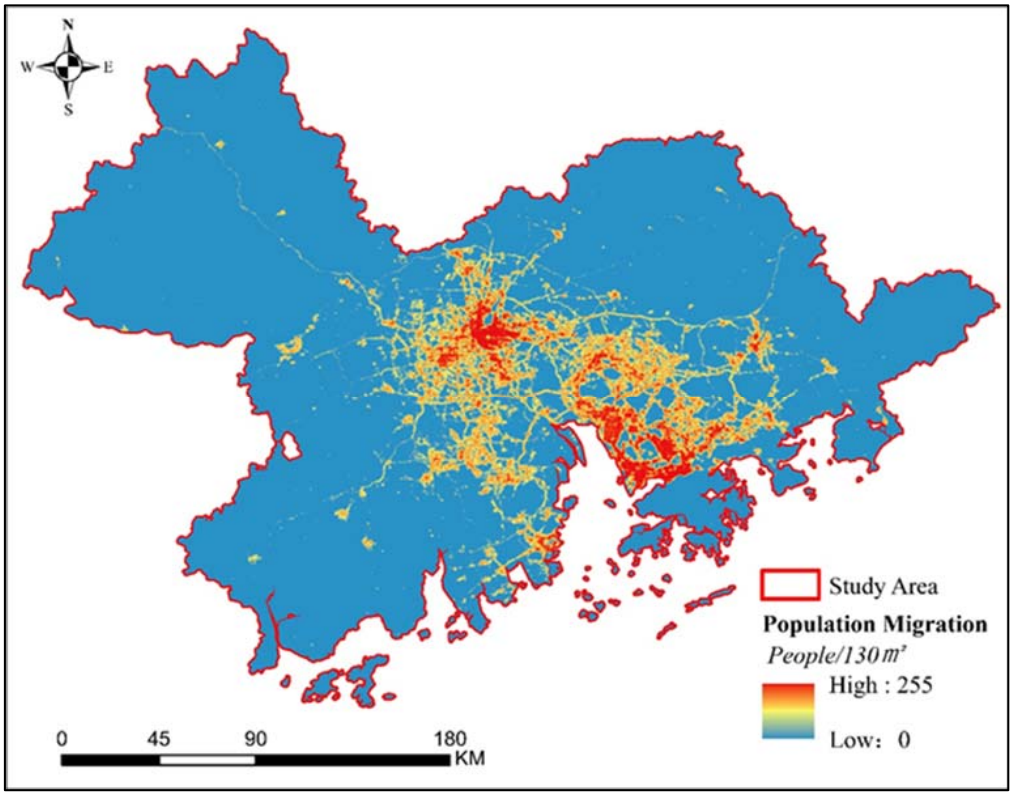

Figure 4. Preprocessing result of population migration data.

Table 1. Details of analyzed data.

Analyzed Data	Spatial Resolution	Data Source	Accessed Time
Luojia-01	130 m × 130 m	http://59.175.109.173:8888/	October 2018–March 2019
POI	—	www.amap.com	January 2021
Population migration	25 m × 25 m	https://heat.qq.com/bigdata/index.html	January 2020–December 2020

2.3. Study Method

2.3.1. Wavelet Transform (WT)

Wavelet transform is an image algorithm based on pixel scale, which can fully consider the interaction relationship between time and frequency in the process of image fusion. Through a time, observation window that changes with frequency, the local properties of time and frequency are amplified to obtain the local features of data [43]. Compared with other algorithms, wavelet transform can decompose data into several independent time and frequency parts without losing the information in the original data [44]. The formula for wavelet transform is as follows:

$$WT(\alpha,\tau) = f(t)\varphi(t) = \frac{1}{\sqrt{\alpha}} f(t) \int_{-\infty}^{+\infty} \varphi\left(\frac{t-b}{\alpha}\right) dt \quad (1)$$

where $f(t)$ is the signal vector of the image, $\varphi(t)$ is the wavelet transform function, α is the wavelet transform scale, τ is the translation of the image signal, and b is the parameters. Scale α (positive) controls the longitudinal scaling of the wavelet function, and τ (which can be positive or negative) controls the translation of the wavelet function, that is, the scale corresponds to the frequency, and the translation corresponds to the time. Different α produces different frequency components, while τ enables the wavelet to perform traversal analysis along the time axis. The meaning of wavelet transform is to shift the basic wavelet function τ and then inner product it with the analysis signal $f(t)$ at different scales α.

2.3.2. Spectral Difference Segmentation (SDS)

Spectral difference segmentation is an image optimization method. Based on image fusion, SDS determines whether to merge objects by judging and analyzing whether the differences between adjacent fused objects meet a given threshold [45]. After merging the fused images, SDS improves the fusion effect [46]. After normalizing the weights of the bands, the spectral difference segmentation formula is:

$$S_{diff} = \frac{\sum_k w_k}{w}\left(\frac{1}{n}\sum_n b_n - \frac{1}{m}\sum_m b_m\right) \quad (2)$$

where, S_{diff} is the spectral difference value of adjacent objects, k is the number of bands, w_k is the weight of the kth band, w is the sum of the band weights, n and m are the total numbers of pixels in adjacent objects, and b_n and b_m is the gray value of the nth and mth pixels in adjacent objects, respectively. S_{diff} is the only parameter used in the spectral difference segmentation algorithm. The larger the value is, the easier it is to merge adjacent objects.

2.3.3. Clustering and Outlier Analysis

As the spatial differences between the main central area of the urban agglomeration and other regions are significant and clusters and outliers reflect the degree of difference between a single geographic unit and other geographic units [47,48], this study used clusters and outliers to identify the main center of the urban agglomeration in the GBA. The formula for clustering and outlier analysis is:

$$I_i = \frac{x_i - \overline{x}}{S_2^i} \sum_{j=1, j\neq i}^{n} w_{ij}(x_i - \overline{x}) \quad (3)$$

where, I_i is the number of statistical points of i for clustering and outlier analysis, w_{ij} is the spatial weight matrix, x_i is the attribute value of i, $\overline{x}$ is the average value of all attribute values, and S_i^2 is the variance of all samples:

$$S_i^2 = \frac{\sum_{j=1,j\neq i}^{n}(x_i - \overline{x})}{n-1} - \overline{x}^2 \tag{4}$$

Normalization of the spatial weights matrix w_{ij}:

$$\sum_{i=1}^{n}\sum_{j\neq i}^{n} w_{ij} = n \tag{5}$$

Introduce Z score to represent statistics with similar values in I_i

$$Z(I_i) = \frac{I_i - E(I_i)}{\sqrt{Var(I_i)}} \tag{6}$$

where (I_i):

$$E(I_i) = -\frac{\sum_{j=1,j\neq i}^{n} w_{ij}}{n-1} \tag{7}$$

$$Var(I_i) = E\left(I_2^i\right) - E(I_i)^2 \tag{8}$$

The final analysis output includes H-H, H-L, L-H, and L-L four kinds of clusters, and all the H-H cluster areas represent the main center of urban agglomeration.

2.3.4. Geographically Weighted Regression (GWR)

Urban centers are considered to have relatively high urban activity density. The urban activity density of different subcenters has a significant relationship with the distance between the subcenter to the main center, which manifests as the closer to the main center, the higher the density of urban activity [49]. This study used geographically weighted regression analysis (GWR) to identify urban agglomeration centers [50], and the formula for GWR analysis is:

$$y_i = \beta_0(\mu_i, v_i) + \sum_{j=1}^{k}\beta_j(\mu_i, v_i)x_{ij} + \varepsilon_i \tag{9}$$

where y_i is urban activity density, μ_i, v_i are the spatial center, $\beta_0(\mu_i, v_i)$ is the intercept, $\beta_k(\mu_i, v_i)$ is the local estimation coefficient, and ε_i is the residual.

3. Results

3.1. Fusion of Multi-Source Big Data

Data fusion integrates data obtained for the same target or the same area in different ways. The fused data can reflect the characteristics of various data, improve the efficiency and effectiveness of data after data fusion, and achieve a better understanding of the target area. Nighttime light data, POI data, and population migration data have a solid spatial relationship in urban space, manifesting as the gradual decrease in nighttime light value from the city center to the city edge, the decline in the number of POIs, and the reduction in population migration. Therefore, nighttime light data, POI data, and population migration data can be fused in urban space [51].

In the wavelet transformation of different images, the original data images of nighttime lights, POI, and population migration can be regarded as a two-dimensional signal matrix, assuming that the size of the matrix is N × N and there are N = 2ˆn (n is a non-negative integer) image signals. Each wavelet transformation decomposes a two-dimensional signal matrix into four two-dimensional signal matrices of 1/4 of the original signal matrix. Each signal matrix contains different frequency bands (HH, HL, LH, LL) corresponding to new wavelet coefficients (equivalent to sampling the horizontal and vertical directions of the original two-dimensional signal matrix at intervals). The wavelet coefficients corresponding to HH represent the diagonal edge characteristics of the image, the wavelet coefficients

corresponding to HL represent the horizontal direction characteristics, and the wavelet coefficients corresponding to LH represent the vertical direction characteristics. After wavelet transformation, the data's horizontal frequency components, vertical frequency components, and diagonal frequency components were obtained. Then, we compared the details of different data in the wavelet transform domain and performed inverse transformation to obtain the final fused data. The flowchart of wavelet transform data fusion is shown in Figure 5.

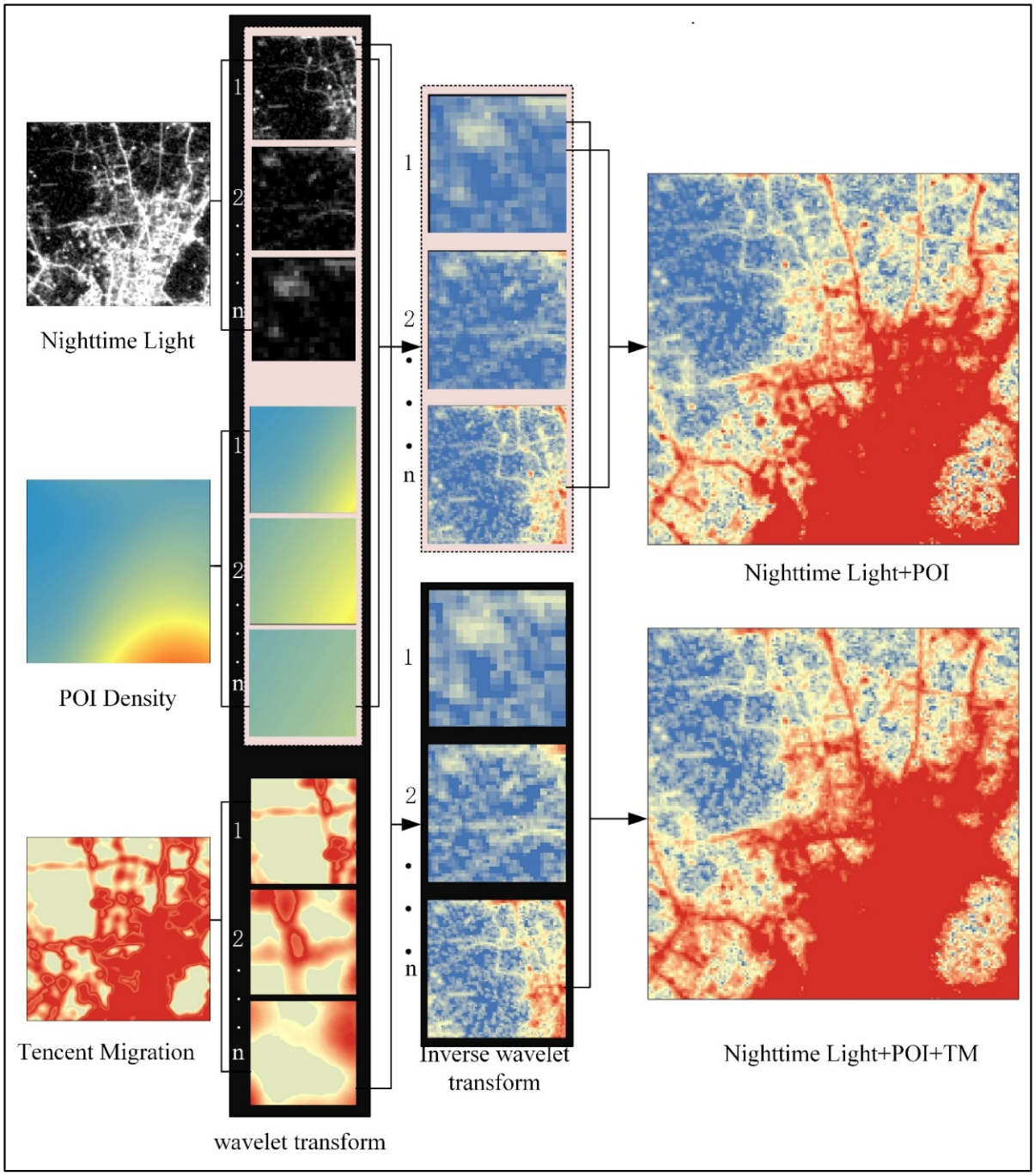

Figure 5. The fusion process of multi-source big data.

Comparing the three different datasets, the distribution of values of POI data and population migration data in the urban agglomeration area is similar to that of nighttime lights. The high values are mainly concentrated in Guangzhou, Shenzhen, Dongguan, and Hong Kong, and the low values are mainly distributed in Zhaoqing, Jiangmen, and

Huizhou, indicating that POI and population migration data can reflect the urban spatial structure as accurately as nighttime light data. Nighttime lights identify the urban center by the nighttime light value of the area, which may be inaccurate to a certain extent. For example, areas with high nighttime light values, such as airports, ports, and power plants, are not the urban center. POI data can represent urban infrastructure construction through their quantitative distribution. Infrastructure construction in airports, ports and other places is significantly different from urban centers. Therefore, fusing POI data with nighttime light data can help correct certain areas' brightness. The nighttime light and POI data show the city's static space, so the city's inner space appears fragmented. The population migration data express the population flow between and within cities. Therefore, fusing the population migration data strengthens the connection between and within cities, thus better representing dynamic urban space.

Although nighttime light data, POI data, and population migration data can all describe the urban spatial structure, some misrepresentations of nighttime light differences affect the identification of the urban center. Fusing the POI data with the nighttime light data can help correct the brightness difference of nighttime lights. Population migration data can strengthen the spatial connection between and within urban areas through population movement. In addition, the fusion of population migration data helps to supplement the spatial details between and within urban agglomerations.

3.2. The Identification of Poly-Centers in the GBA

This study used the spatial differences between urban spaces with different urban development and spatial structures to identify urban centers. Nighttime lights, POIs, and population migration data express different aspects of urban spatial differences. For nighttime light data, the urban center has high nighttime light values, while the non-central areas have relatively low values. For POIs, POIs are highly concentrated in the urban center and scattered in non-central areas. For population migration data, population migration is prominent in the central urban areas and minor in the non-urban areas.

Only certain parts of the area can be defined as urban centers in a city or metropolis. Therefore, it is essential to define urban centers quantitatively. Based on existing research on urban center identification, we propose four indicators to determine the city center. To be determined as urban centers, the areas need to satisfy the following four indicators simultaneously (Table 2).

Table 2. Urban center identification indicators.

Indicators	Equation	Urban Center	Non Urban Center	Definition
Area	$S = N \times CS$	≥ 15 km^2	< 15 km^2	N is the number of pixels; CS is the pixel size
Density standard deviation	$STD = \sqrt{\frac{1}{N}\sum_{i=1}^{N}(x_i - \overline{x})^2}$	>0	≈0	x_i is the value of ith pixel, $\overline{x}$ is the average value of pixels
Compactness index	$CI = 4\pi S/P^2$	Close to 1	Close to 0	P is the perimeter of the city center
Elongation ratio	$ELG = LEN/WID$	<3	≥ 3	LEN and WID are the major and minor axes of the minimum bounding rectangle in the city center, respectively

The area is the identified metropolitan area in the urban center identification index [52]. According to the existing study on urban center identification, the minimum size of the first-tier urban center in China is 15 km^2, and the urban center area of an ordinary city is no less than 5 km^2. Therefore, this study selected 15 km^2 as the minimum area of the urban center in the GBA [26]. The density standard deviation is a measure of how scattered the pixels are. A larger standard deviation means that most of the values in the pixel are different from the average. The purpose of using the standard deviation is to remove some high pixel values that cannot be considered urban centers (such as airports, ports, and

power plants with high pixel values). The value of the compactness index ranges from 0 to 1. The smaller the compactness index, the less compact and scattered the shape of the area, and the urban center should be more compact than the non-urban center. The elongation ratio aims to eliminate the urban center formed by narrow roads. By comparing a large number of elongation-ratio-related studies, we found that the urban center elongation ratio formed by narrow roads is greater than 3 [53]. The identification process of the city center in the GBA is shown in Figure 6.

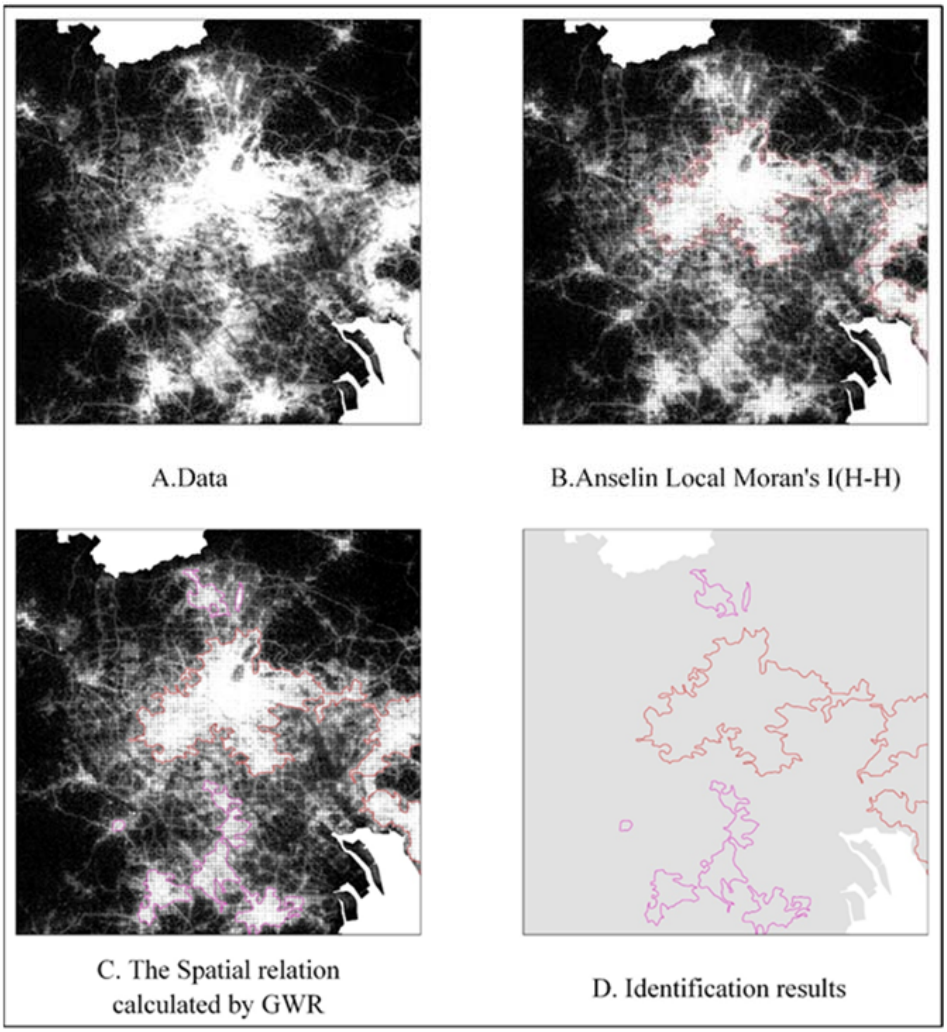

Figure 6. Flowchart of urban center identification.

The identified urban agglomeration center of the GBA based on nighttime light data analysis and urban center identification index constraints is shown in Figure 7. The urban center area is 2222.89 km^2 and includes Guangzhou, Shenzhen, Hong Kong, Zhuhai, Macau, and other places, accounting for 3.97% of the total administrative area. The urban centers identified by nighttime lights show that Guangzhou, Shenzhen, and Hong Kong, as super-first-tier cities, play a dominant role in the development of the GBA, and the extent of these urban centers far exceeds that of Zhuhai, Hong Kong, Foshan, and other urban centers. The urban center area identified by nighttime lights depends on the level of the nighttime light brightness value. The area with the high light brightness value and an extensive range is recognized as the urban center, while the area with the low light brightness value is not recognized as the city center range. However, areas including Baiyun International Airport and Nansha Port were also identified as urban centers, showing the limitations of solely relying on nighttime light data.

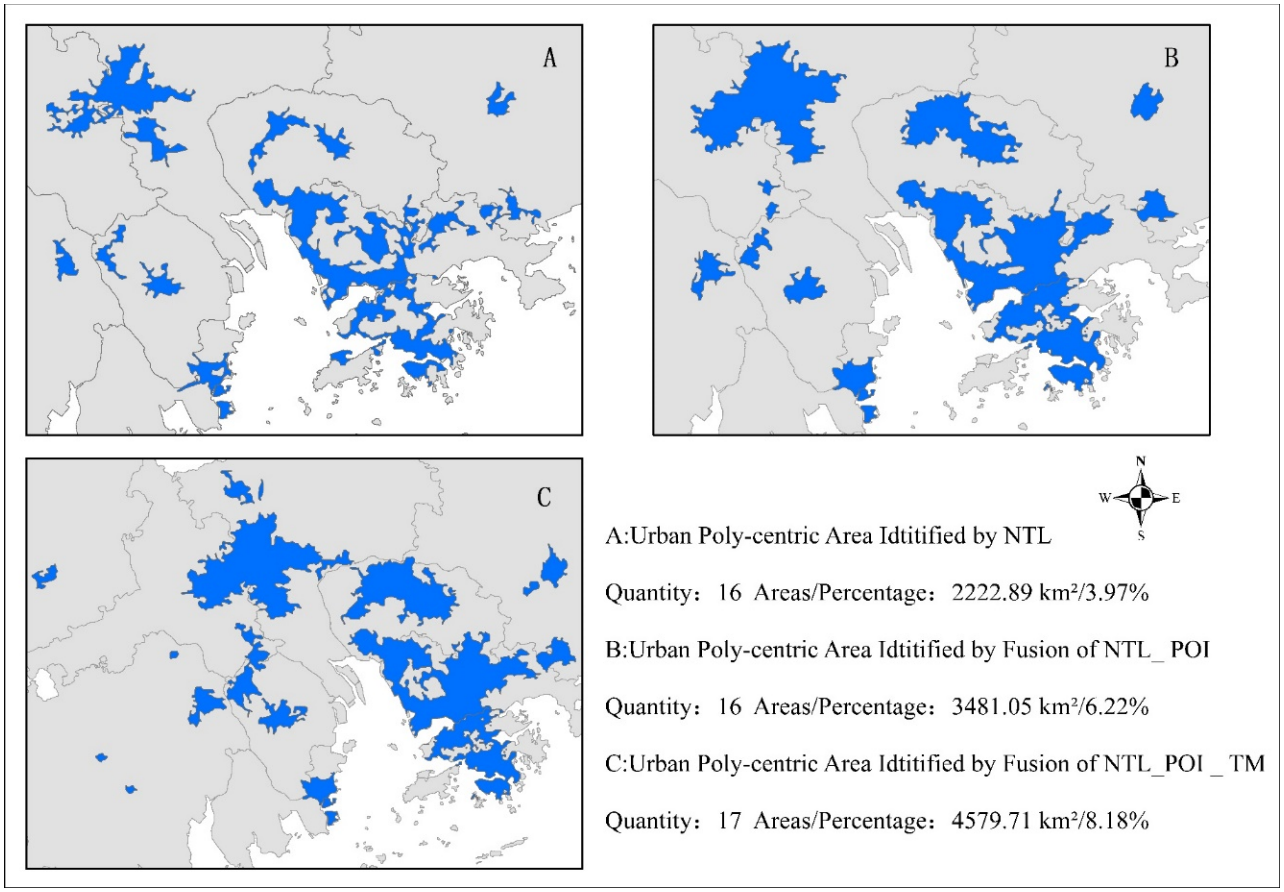

Figure 7. The identification results of polycentric spatial structure in the GBA.

After the fusion of nighttime light data and POI data, the high values are mainly clustered in Guangzhou, Foshan, Shenzhen, Zhuhai, Hong Kong, and Macau. Among them, Guangzhou, Foshan, Shenzhen, Hong Kong, Macau, and Zhuhai show a trend of integrated development, which is in line with the current state of urban development in the GBA. The urban center area identified after the fusion of nighttime light and POI data is 3481.05 km^2, mainly concentrated in Guangzhou, Foshan, Shenzhen, Hong Kong, Macau, Zhuhai, Dongguan, and Shunde, accounting for 6.22% of the total administrative area. The results of the urban center identified by fusing with the POI data showed similar results with solely nighttime light data analysis but have a wider extent—identifying the Shunde urban center. Fusing the POI data corrects the false urban center areas with high nighttime brightness values. After fusing POI data, the areas with a single high nighttime brightness value, such as Baiyun International Airport and Nansha Port, were not identified as urban centers. The newly identified urban centers had lights. The newly identified urban center has the dual characteristics of high light value and a high number of POI.

Nighttime light and POI data represent the development level of urban areas, the distribution trend of urban infrastructure, etc., but focus on static space and fragmented structures. There are also dynamic spatial connections between and within cities in urban agglomerations—this connection includes the mutual flow of population, information, and materials. Therefore, the static urban space represented by nighttime light data and POIs cannot fully reflect this dynamic connection. Fusing the population data based on nighttime light data and POI data fusion, the urban center area identified is 4579.71 km^2, accounting for 8.18% of the total area of the urban center administrative district. The extent of the urban center has increased significantly. This method also identified a small number of urban centers in new airport cities, where there is a large volume of population migration and cities in the east and west of the GBA with a lower level of development. The mechanism

behind this is that the urban subcenters share the population burden of the main city center. The population migration forms urban subcenters in cities, such as Kaiping, Huidong, and new airport cities. The spatial structure of newly identified urban centers in the GBA shows an integrated development trend in Guangzhou, Foshan, Shenzhen, Hong Kong, Macau, and Zhuhai, which is in line with the planning of the GBA.

3.3. Validation of Identification Results

Urban centers rarely have detailed scope and definition in planning documents and are more part of a widely recognized subjective will. Therefore, the lack of a gold standard of urban centers makes validating identified urban centers challenging. Existing studies have shown a significant spatial correlation between population distribution and urban centers—urban centers are often the centers of large population clusters [54,55]. Therefore, this study used the clustering distribution populations obtained from the permanent population spatial distribution data in the GBA at the end of 2020 to validate the results of the identified urban center using a consistency test. The permanent resident population spatial distribution data are from statistical data, acknowledged by the academic community as the gold standard of population data. The consistency test results are shown in Table 3.

Table 3. The validation result of urban center identification in the GBA.

Validation Indicators	Nighttime Light	Nighttime Light + POI	Nighttime Light + POI + Population Migration
Accuracy	78.13%	87.37%	93.22%
Kappa	0.6637	0.7961	0.8744

Table 3 shows that the accuracy of nighttime light identified urban centers is 78.13%, and the Kappa coefficient is 0.6637; the accuracy of nighttime light and POI identified urban centers is 87.37%, and the Kappa coefficient is 0.7961; and the accuracy of nighttime light, POI, and population migration data fused identified urban centers is 93.22%, and the Kappa coefficient is 0.8744. Single nighttime light data have the lowest accuracy in identifying urban poly-centers, and the identification accuracy significantly improved after correcting nighttime lights by integrating POI data. Additionally, integrating population migration data strengthened the internal spatial connection of urban agglomerations and identified urban poly-centers with the highest accuracy.

3.4. Hierarchy Evaluation of the Identified Urban Poly-Centers

The proposed development plan of the GBA aims to build the GBA into a high-ranking world-class bay area and metropolis. The planned urban agglomeration spatial structure planning exhibits "four regional main centers, one regional subcenter, six local main centers, and several local subcenters". In addition, it plans three spatial development arteries: Guangzhou–Foshan, Shenzhen–Hong Kong, and Zhuhai–Macau (Figure 8). In the development plan, the leading regional centers are Guangzhou, Shenzhen, Hong Kong, and Macau, and the subregional center is Zhuhai. The leading local centers are Zhaoqing, Foshan, Zhongshan, Jiangmen, Dongguan, and Huizhou. The comparison results of the identified poly-centers of the GBA in this study and the poly-centers proposed in the GBA development plan are shown in Figure 8. The number of urban centers identified in this study is consistent with the number of centers proposed in the development plan. From the perspective of the central development arteries, the integrated development trend of Guangzhou and Foshan is noticeable. The urban centers of Shenzhen and Hong Kong have also been connected. In contrast, the integrated development trend of Zhuhai and Macao urban centers is relatively weak, which is consistent with the development plan outline of the GBA.

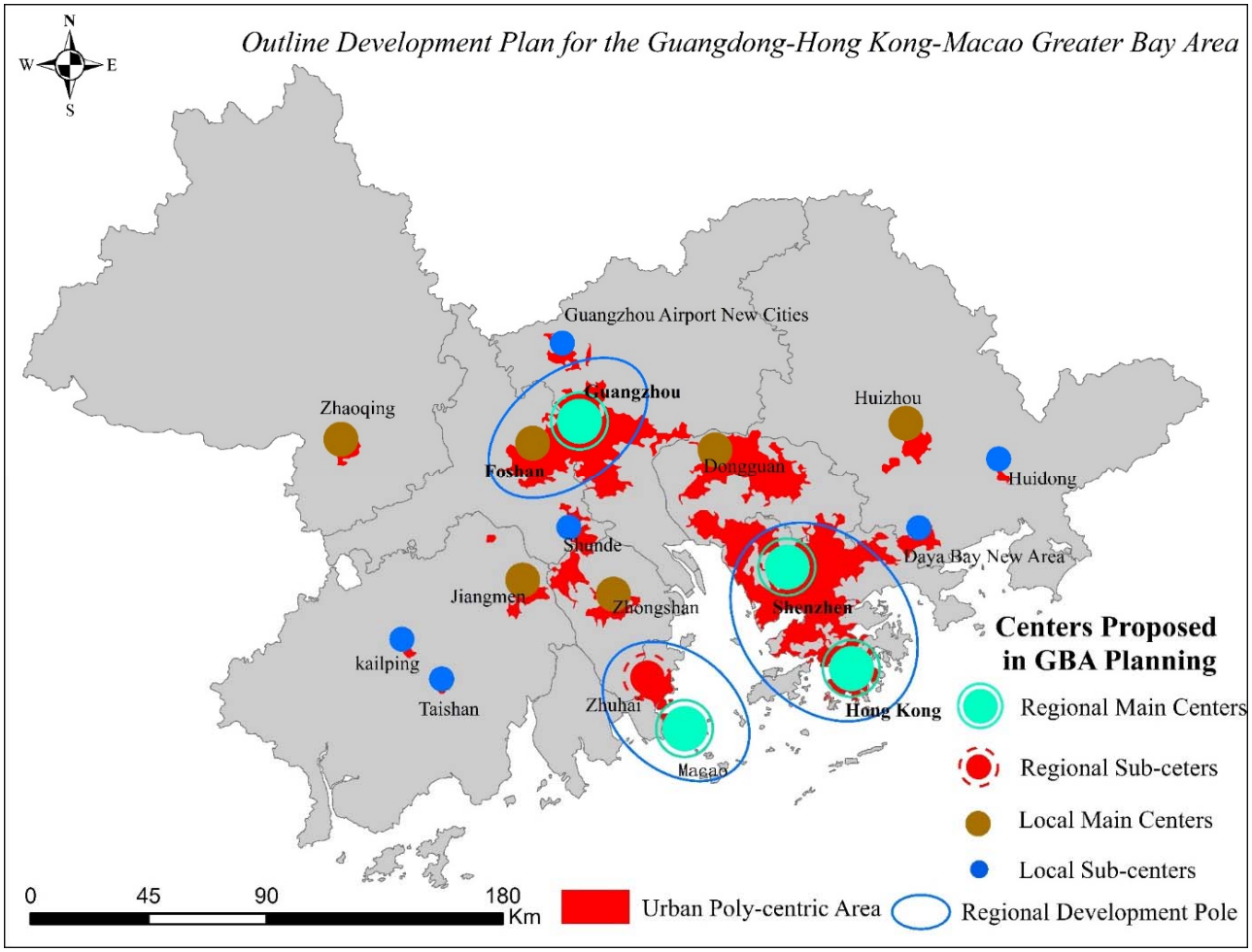

Figure 8. Comparison between identified urban poly-center and that proposed in the GBA development planning.

In terms of spatial distribution, the identified urban poly-centers in the GBA are generally consistent with the centers proposed in the development plan outline. However, development differences between and within main and subcenters lead to the same urban centers belonging to the same categories having different development levels and hierarchies. As we cannot observe and determine the hierarchy level of urban centers by their spatial extent, we need to evaluate their hierarchy level from quantitative measurement methods. Evaluating the hierarchy level of urban poly-centers can provide planning and management authorities insights to allocate urban resources better. Therefore, based on the GBA metropolis's urban poly-center identification results, this study further evaluates the development level of different urban centers based on their spatial heterogeneity. According to the natural city method, nighttime light data follow a heavy-tailed distribution (that is, there are many pixels with low values). The head-to-tail segmentation identifies the urban center (the head refers to the pixels with values higher than the average). Iterating head-to-tail segmentation can identify the places with the highest pixel values as urban centers, which is more reliable than the bisection method [56].

After determining the poly-centers of the GBA, there are apparent differences in morphology and development between identified urban centers. We performed iterative calculations on different identified urban centers based on the natural city method through clustering and outliers. Assuming that the identified city center indices are all 1, we increased the center index by one each time we iteratively calculate the H-H clustering until there was no obvious spatial difference. Figure 9 shows the urban poly-center hierarchical level evaluation process of the GBA.

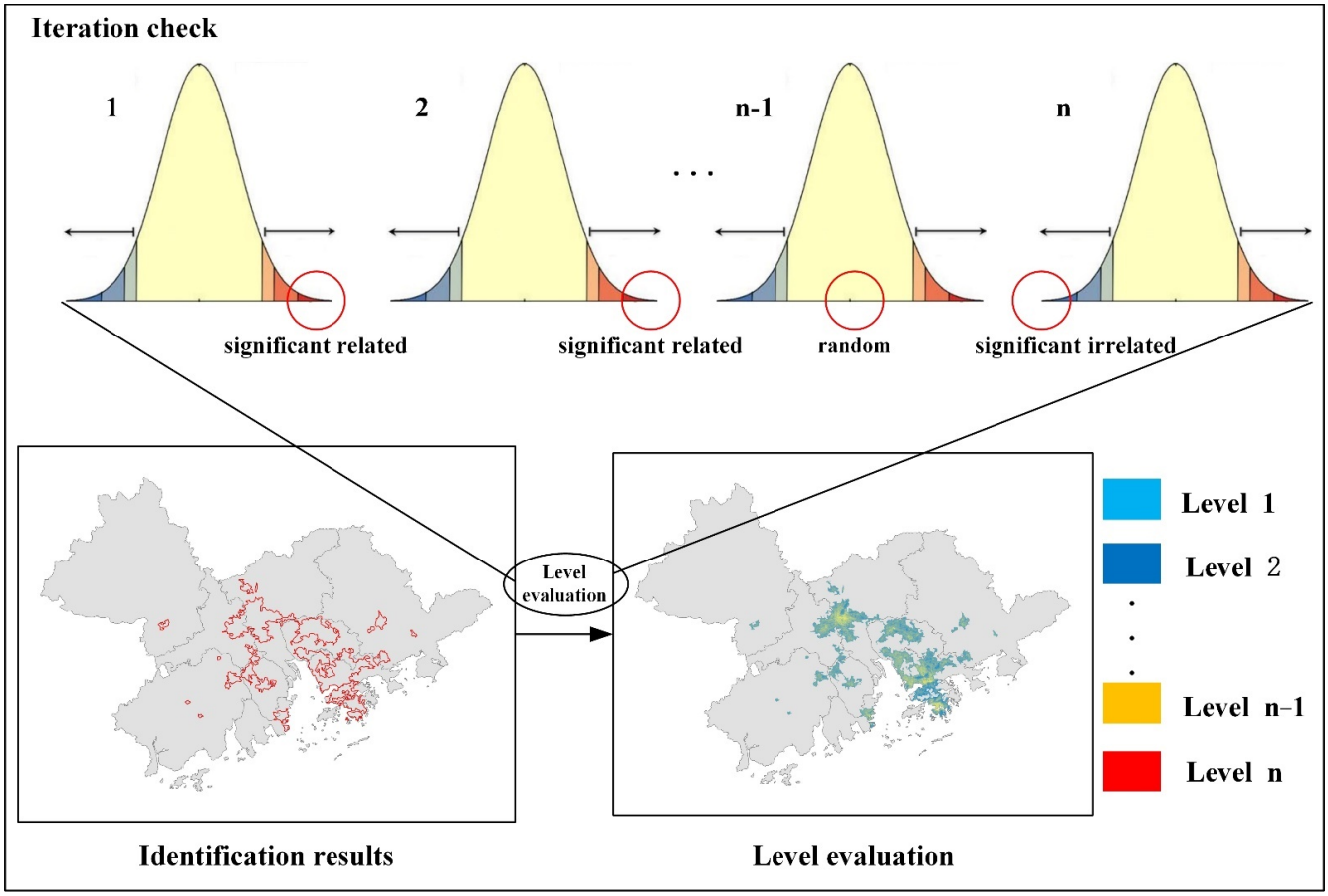

Figure 9. The working flow of the urban poly-center hierarchical level evaluation process.

Referring to the method of evaluating urban poly-centers in the natural city, cluster analysis, and outlier analysis were used to evaluate the center levels of the GBA. The main center levels of urban regions were obtained as shown in Figure 10, and the highest, lowest, and average levels of different urban centers are shown in Table 4. The highest levels of urban centers in the four regional main centers of Hong Kong, Macao, Guangzhou, and Shenzhen are 7, 5, 10, and 9, respectively, the highest level of urban centers in Zhuhai is 10, and the highest levels of urban centers in the other six regional sub-centers of Foshan, Huizhou, Dongguan, Zhongshan, Jiangmen, and Zhaoqing are 5, 4, 7, 6, 5, and 5, respectively. From the perspective of the urban center level, the primary and secondary order of urban multi-centers in the GBA should be Guangzhou, Shenzhen, Hong Kong, Zhuhai, Dongguan, Zhongshan, Foshan, Zhaoqing, Macao, Jiangmen, and Huizhou. As can be seen, the obtained evaluation results of the multi-center level of the GBA are quite different from those proposed in the GBA Development Plan.

The GBA development plan outline categorizes Hong Kong, Macau, Guangzhou, and Shenzhen as the regional main centers. Still, our evaluation of the urban center level shows that Guangzhou has the highest level of the urban center, followed by Shenzhen. Although Hong Kong and Macao serve as the Asian international financial center and international free port, respectively, and are planned as the regional main center in the development plan outline, the development level of these two cities is lower than Guangzhou and Shenzhen. It is equivalent to the level of Zhuhai, Foshan, and other regions, which are cities planned as secondary regional centers in the plan outline. The reason behind this discrepancy is that, on the one hand, Hong Kong and Macao play a critical role in the development plan outline due to their positions of functioning as essential gateways for international trade. On the other hand, urban development has achieved great success in mainland China, especially in the Pearl River Delta region.

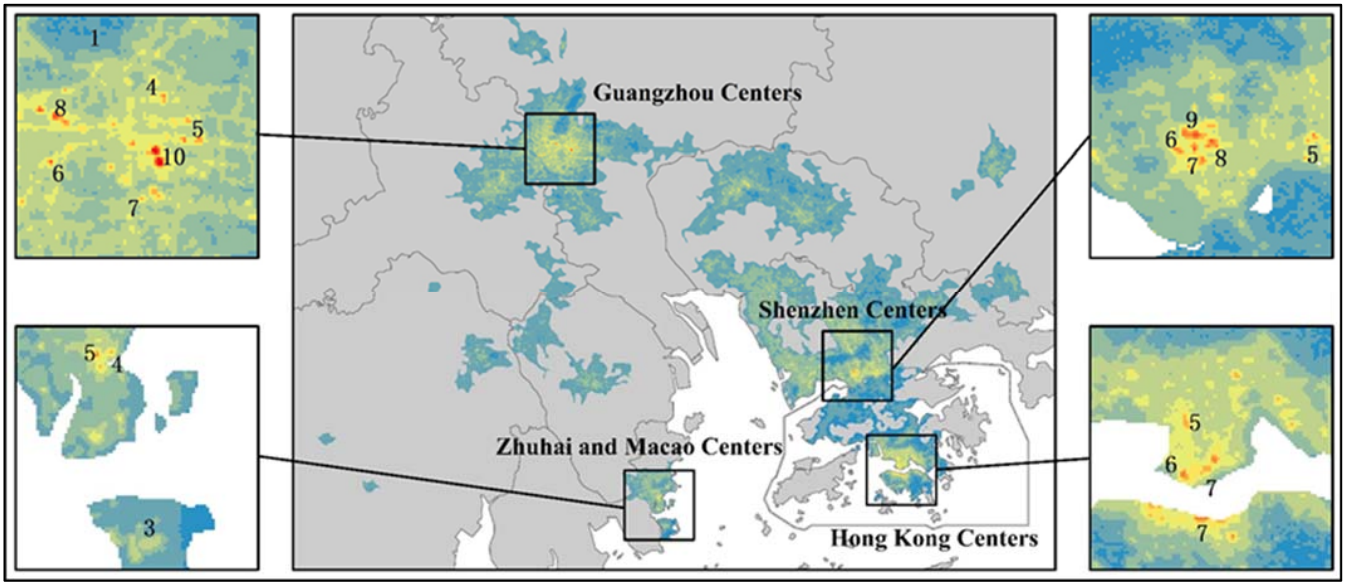

Figure 10. Evaluation results of urban poly-center hierarchical level (the numbers in the figure indicate the hierarchy of urban centers).

Table 4. The hierarchical level evaluation of the urban poly-centers.

Cities and Development Corridors	The Highest Hierarchy of Urban Center	The Lowest Hierarchy of Urban Center	The Average Level of Urban Center
Hong Kong	7	3	5
Macau	5	2	3.5
Guangzhou	10	3	6
Shenzhen	9	3	5.4
Zhuhai	7	2	3
Dongguan	7	2	3
Zhongshan	6	2	3.3
Foshan	5	1	1.8
Huizhou	4	1	1.5
Zhaoqing	5	1	2
Jiangmen	5	1	1.6
Hong Kong-Shenzhen Development Corridor	9	3	3.2
Macau-Zhuhai Development Corridor	7	2	2.4
Guangzhou-Foshan Development Corridor	10	1	4

4. Discussion

The traditional identification and evaluation of the urban centers mainly rely on statistical survey data and remote sensing data. The use of statistical survey data suffers from subjectivity and irreproducibility, and remote sensing data such as nighttime light data are often interfered with by the data itself, such as the spillover effect of lights [57]. Therefore, to the best of our knowledge, there is a lack of scientific, objective, and straightforward methods to evaluate the heterogeneous spatial development of urban agglomerations. We first used the wavelet transform to fuse nighttime light, POI, and population migration. Second, we conducted clustering and outlier analysis and GWR to identify and grade the urban poly-centers in the GBA. This study explored a reliable and straightforward urban center identification and grade evaluation workflow. It provides an objective method to evaluate urban development in the GBA.

As commonly used data for urban center identification, nighttime light data can directly reflect the development level difference among urban areas through light intensity. They then can determine the extent of the urban center, which is the key to urban center identification [58]. However, the nighttime light data's limitations, such as the light spillover

effect, resulted in some unsatisfactory recognition results [59]. Later, scholars explored and discovered the strong spatial correlation between POI data and nighttime light data and tried to use POI data to correct the errors caused by nighttime light data. The method that fused the POI and nighttime light data achieved a better urban center identification result [60]. The nighttime light data and POI data only show the static aspect of urban space, while the urban agglomeration is dynamic between and within cities and districts [61]. Therefore, this study contributes to the existing studies on evaluating the urban spatial development by integrating nighttime light, POI, and population migration data, and taking both dynamic and static elements of urban space into account [62].

Urban polycentric spatial structure identification lays the foundation for urban agglomeration spatial optimization research. However, only the number and extent of identified urban poly-centers cannot directly reflect the urban development level. For example, in the rapid development of cities, multiple urban centers may expand and merge into a larger urban center. Although the number of urban centers decreases, the level of urban development increases [63,64]. Therefore, it is necessary to further evaluate the hierarchy of different urban centers to accurately understand the current status of urban development [65]. The poly-center hierarchical evaluation in this study does not stop at identifying the primary and sub-centers. Instead, it can accurately grade the level of each urban center based on urban center identification. Our study has high application prospects and is relatively straightforward to compute compared with the existing research [66]. Our results on the development status of the GBA's urban poly-centers can shed light on guiding the spatial development of urban agglomerations.

Compared with other multi-source big data fusion models, this study uses wavelet transform to perform multi-resolution and multi-scale transformation and fusion of different data, which maximizes the effect of data fusion while maintaining different data characteristics [30,67,68]. Additionally, this study uses SDS to optimize and adjust the fused images, and fuses them by using the spectral differences of adjacent pixels, which further improves the effect of data fusion [69,70]. The data fusion method proposed in this study is not only simple to operate, and easy to apply in a wide range, but also has low noise and a small amount of redundant data after fusion, which has not been achieved by the data fusion methods proposed in other studies [71–73].

Despite this, our analysis results suffer from the limitation of neglecting the heterogeneous urban functions among cities. For example, although some identified urban centers belong to the same hierarchical level, such as the urban centers in Macau and Foshan, the two urban centers have different urban functions [74]. Secondly, there are some uncertainties in the data used in this study, especially POI data and population migration data. To some extent, these two data are only the abstract simulation of different elements in the virtual geographical space, which is still different from the actual development of urban spatial elements and the spatial flow of population elements. Therefore, in the next study, not only can the functions of urban centers of the same level be classified and continuously discussed, but also the spatial registration of POI data and population migration data with the actual urban space and population flow can be carried out to further improve the data quality. Finally, this study puts forward a feasible method to identify and evaluate urban polycentric, which has certain guiding significance for future urban polycentric identification and evaluation.

5. Conclusions

As the polycentric spatial structure is an inevitable choice for rapid urban development, it is essential for urban planners to identify and evaluate the polycentric spatial structure of existing urban agglomerations. Using nighttime light, POI data, and population migration data, we identified an area of 4579.81 km^2 of urban poly-centers of the GBA, accounting for 8.18% of the total administrative area with a recognition accuracy of 93.22% and the Kappa coefficient of 0.8744. The number and extent of the identified multi-centers are consistent with the development plan outline for the GBA. As for the hierarchy of different

urban centers, Guangzhou, Shenzhen, Hong Kong, Zhuhai, Dongguan, Zhongshan, Foshan, Zhaoqing, Macao, Jiangmen, and Huizhou rank from the highest to the lowest in the urban center hierarchy.

The evaluation result differs from the development plan outline, showing that the actual development level of the GBA is different from the proposed planning. This study puts forward a new method to identify and evaluate the urban polycentric spatial structure, adding objectivity and robustness to urban centers' identification and evaluation that previously relied solely on subjective judgment. Our results on the spatial development of the GBA can provide realistic guidance for future urban planning and regional development plans.

Author Contributions: Conceptualization, X.H. and Y.Z. (Yuquan Zhou); methodology, X.H. and Y.Z. (Yuquan Zhou); software, X.H. and Y.Z. (Yuquan Zhou); validation, X.H., Y.Z. (Yuquan Zhou), and Y.Z. (Yiting Zhu); formal analysis, X.H.; investigation, Y.Z. (Yuquan Zhou); resources, Y.Z. (Yuquan Zhou); data curation, X.H.; writing—original draft preparation, X.H., Y.Z. (Yuquan Zhou) and Y.Z. (Yiting Zhu); writing—review and editing, X.H., Y.Z. (Yuquan Zhou) and Y.Z. (Yiting Zhu); X.H. has contributed equally to this work and share first authorship. All authors have read and agreed to the published version of the manuscript.

Funding: This research received no external funding.

Institutional Review Board Statement: Not applicable.

Informed Consent Statement: Not applicable.

Data Availability Statement: The data presented in this study are publicly available data sources stated in the citation. Please contact the corresponding author regarding data availability.

Acknowledgments: Thanks to all editors and reviewers.

Conflicts of Interest: The authors declare no conflict of interest.

References

1. Dong, L.; Longwu, L.; Zhenbo, W.; Liangkan, C.; Faming, Z. Exploration of Coupling Effects in the Economy–Society–Environment System in Urban Areas: Case Study of the Yangtze River Delta Urban Agglomeration. *Ecol. Indic.* **2021**, *128*, 107858. [CrossRef]
2. Li, X.; Li, Y.P.; Huang, G.H.; Lv, J.; Ma, Y. A Multi-Scenario Input-Output Economy-Energy-Environment Nexus Management Model for Pearl River Delta Urban Agglomeration. *J. Clean. Prod.* **2021**, *317*, 128402. [CrossRef]
3. Mou, J. Extracting Network Patterns of Tourist Flows in an Urban Agglomeration Through Digital Footprints: The Case of Greater Bay Area. *IEEE Access* **2022**, *10*, 16644–16654. [CrossRef]
4. Abozeid, A.S.M.; AboElatta, T.A. Polycentric vs Monocentric Urban Structure Contribution to National Development. *J. Eng. Appl. Sci.* **2021**, *68*, 11. [CrossRef]
5. Wang, J.; Dong, W. Multiple Effects of Urban Innovation Activities on Growth of Key Industries: Case Study in Hangzhou, China. *J. Urban Plan. Dev.* **2022**, *148*, 05021054. [CrossRef]
6. Xu, R.; Yang, G.; Qu, Z.; Chen, Y.; Liu, J.; Shang, L.; Liu, S.; Ge, Y.; Chang, J. City Components–Area Relationship and Diversity Pattern: Towards a Better Understanding of Urban Structure. *Sustain. Cities Soc.* **2020**, *60*, 102272. [CrossRef]
7. Yang, S.; Myung, J. Morphological Adaptation Types of Small-industrial Clusters to Traditional Urban Tissue—The 2000s' Gold Jewelry Manufacturing in Seoul CBD, Korea. *J. Asian Arch. Build. Eng.* **2017**, *16*, 15–21. [CrossRef]
8. Ma, M.; Liu, S.; Su, M.; Wang, C.; Ying, Z.; Huo, M.; Lin, Y.; Yang, W. Spatial Distribution and Potential Sources of Microplastics in the Songhua River Flowing through Urban Centers in Northeast China. *Environ. Pollut.* **2022**, *292*, 118384. [CrossRef]
9. Kwan, S.C.; Saragih, I.J. Urban Environment and Cause Specific Visits to Community Health Centers of Medan City, Indonesia in 2016. *Sustain. Cities Soc.* **2020**, *59*, 102228. [CrossRef]
10. Zhou, F.; Zhang, B. Detecting and Visualizing the Communities of Innovation in Beijing-Tianjin-Hebei Urban Agglomeration Based on the Patent Cooperation Network. *Complexity* **2021**, *2021*, 5354170. [CrossRef]
11. Ma, H.; Xu, X. Knowledge Polycentricity of China's Urban Agglomerations. *J. Urban Plan. Dev.* **2022**, *148*, 04022014. [CrossRef]
12. McMillen, D.P. Nonparametric Employment Subcenter Identification. *J. Urban Econ.* **2001**, *50*, 448–473. [CrossRef]
13. Redfearn, C.L. The Topography of Metropolitan Employment: Identifying Centers of Employment in a Polycentric Urban Area. *J. Urban Econ.* **2007**, *61*, 519–541. [CrossRef]
14. Rao, Y.; Yang, J.; Dai, D.; Wu, K.; He, Q. Urban Growth Pattern and Commuting Efficiency: Empirical Evidence from 100 Chinese Cities. *J. Clean. Prod.* **2021**, *302*, 126994. [CrossRef]
15. McMillen, D.P. Identifying Sub-centres Using Contiguity Matrices. *Urban Stud.* **2003**, *40*, 57–69. [CrossRef]

16. McMillen, D.P. The Return of Centralization to Chicago: Using Repeat Sales to Identify Changes in House Price Distance Gradients. *Reg. Sci. Urban Econ.* **2003**, *33*, 287–304. [CrossRef]
17. Liu, X.; Derudder, B.; Wang, M. Polycentric Urban Development in China: A Multi-Scale Analysis. *Environ. Plan. B Urban Anal. City Sci.* **2018**, *45*, 953–972. [CrossRef]
18. McMillen, D.P. Employment Densities, Spatial Autocorrelation, and Subcenters in Large Metropolitan Areas. *J. Reg. Sci.* **2004**, *44*, 225–244. [CrossRef]
19. Riguelle, F.; Thomas, I.; Verhetsel, A. Measuring Urban Polycentrism: A European Case Study and Its Implications. *J. Econ. Geogr.* **2007**, *7*, 193–215. [CrossRef]
20. Garcia-López, M.À. Population Suburbanization in Barcelona, 1991–2005: Is Its Spatial Structure Changing? *J. Hous. Econ.* **2010**, *19*, 119–132. [CrossRef]
21. Wang, Y.; Shen, Z. Comparing Luojia 1-01 and VIIRS Nighttime Light Data in Detecting Urban Spatial Structure Using a Threshold-Based Kernel Density Estimation. *Remote Sens.* **2021**, *13*, 1574. [CrossRef]
22. He, X.; Zhu, Y.; Chang, P.; Zhou, C. Using Tencent User Location Data to Modify Night-Time Light Data for Delineating Urban Agglomeration Boundaries. *Front. Environ. Sci.* **2022**, *10*, 860365. [CrossRef]
23. Long, Y. Redefining Chinese City System with Emerging New Data. *Appl. Geogr.* **2016**, *75*, 36–48. [CrossRef]
24. Jiang, B.; Liu, X. Scaling of Geographic Space from the Perspective of City and Field Blocks and Using Volunteered Geographic Information. *Int. J. Geogr. Inf. Sci.* **2012**, *26*, 215–229. [CrossRef]
25. Ou, J.; Liu, X.; Liu, P.; Liu, X. Evaluation of Luojia 1-01 Nighttime Light Imagery for Impervious Surface Detection: A Comparison with NPP-VIIRS Nighttime Light Data. *Int. J. Appl. Earth Obs. Geoinf.* **2019**, *81*, 1–12. [CrossRef]
26. Chen, Z.; Yu, B.; Song, W.; Liu, H.; Wu, Q.; Shi, K.; Wu, J. A New Approach for Detecting Urban Centers and Their Spatial Structure with Nighttime Light Remote Sensing. *IEEE Trans. Geosci. Remote Sens.* **2017**, *55*, 6305–6319. [CrossRef]
27. He, X.; Zhou, C.; Wang, Y.; Yuan, X. Risk Assessment and Prediction of COVID-19 Based on Epidemiological Data from Spatiotemporal Geography. *Front. Environ. Sci.* **2021**, *9*, 634156. [CrossRef]
28. Lou, G.; Chen, Q.; He, K.; Zhou, Y.; Shi, Z. Using Nighttime Light Data and POI Big Data to Detect the Urban Centers of Hangzhou. *Remote Sens.* **2019**, *11*, 1821. [CrossRef]
29. Chen, Y.; Yue, W.; La Rosa, D. Which Communities Have Better Accessibility to Green Space? An Investigation into Environmental Inequality Using Big Data. *Landsc. Urban Plan.* **2020**, *204*, 103919. [CrossRef]
30. Zhou, C.; He, X.; Wu, R.; Zhang, G. Using Food Delivery Data to Identify Urban -Rural Areas: A Case Study of Guangzhou, China. *Front. Earth Sci.* **2022**, *10*, 860361. [CrossRef]
31. He, X.; Zhou, C.; Zhang, J.; Yuan, X. Using Wavelet Transforms to Fuse Nighttime Light Data and POI Big Data to Extract Urban Built-Up Areas. *Remote Sens.* **2020**, *12*, 3887. [CrossRef]
32. Liu, J.; Deng, Y.; Wang, Y.; Huang, H.; Du, Q.; Ren, F. Urban Nighttime Leisure Space Mapping with Nighttime Light Images and POI Data. *Remote Sens.* **2020**, *12*, 541. [CrossRef]
33. Wang, L.; Fan, H.; Wang, Y. Improving Population Mapping Using Luojia 1-01 Nighttime Light Image and Location-Based Social Media Data. *Sci. Total Environ.* **2020**, *730*, 139148. [CrossRef]
34. Li, F.; Yan, Q.; Bian, Z.; Liu, B.; Wu, Z. A POI and LST Adjusted NTL Urban Index for Urban Built-Up Area Extraction. *Sensors* **2020**, *20*, 2918. [CrossRef] [PubMed]
35. Wang, M.; Song, Y.; Wang, F.; Meng, Z. Boundary Extraction of Urban Built-Up Area Based on Luminance Value Correction of NTL Image. *IEEE J. Sel. Top. Appl. Earth Obs. Remote Sens.* **2021**, *14*, 7466–7477. [CrossRef]
36. Shi, K.; Chang, Z.; Chen, Z.; Wu, J.; Yu, B. Identifying and Evaluating Poverty Using Multisource Remote Sensing and Point of Interest (POI) Data: A Case Study of Chongqing, China. *J. Clean. Prod.* **2020**, *255*, 120245. [CrossRef]
37. Ma, T. An Estimate of the Pixel-Level Connection between Visible Infrared Imaging Radiometer Suite Day/Night Band (VIIRS DNB) Nighttime Lights and Land Features across China. *Remote Sens.* **2018**, *10*, 723. [CrossRef]
38. Jun, Z.; Xiao-Die, Y.; Han, L. The Extraction of Urban Built-Up Areas by Integrating Night-Time Light and POI Data—A Case Study of Kunming, China. *IEEE Access* **2021**, *9*, 22417–22429. [CrossRef]
39. Zhang, J.; Yuan, X.; Tan, X.; Zhang, X. Delineation of the Urban-Rural Boundary through Data Fusion: Applications to Improve Urban and Rural Environments and Promote Intensive and Healthy Urban Development. *Int. J. Environ. Res. Public Health* **2021**, *18*, 7180. [CrossRef]
40. He, X.; Yuan, X.; Zhang, D.; Zhang, R.; Li, M.; Zhou, C. Delineation of Urban Agglomeration Boundary Based on Multisource Big Data Fusion—A Case Study of Guangdong–Hong Kong–Macao Greater Bay Area (GBA). *Remote Sens.* **2021**, *13*, 1801. [CrossRef]
41. Wu, W.; Zhao, H.; Jiang, S. A Zipf's Law-Based Method for Mapping Urban Areas Using NPP-VIIRS Nighttime Light Data. *Remote Sens.* **2018**, *10*, 130. [CrossRef]
42. Yang, X.; Ye, T.; Zhao, N.; Chen, Q.; Yue, W.; Qi, J.; Zeng, B.; Jia, P. Population Mapping with Multisensor Remote Sensing Images and Point-Of-Interest Data. *Remote Sens.* **2019**, *11*, 574. [CrossRef]
43. Feng, X.; Zhang, W.; Su, X.; Xu, Z. Optical Remote Sensing Image Denoising and Super-Resolution Reconstructing Using Optimized Generative Network in Wavelet Transform Domain. *Remote Sens.* **2021**, *13*, 1858. [CrossRef]
44. Jia, X.; Peng, Y.; Li, J.; Ge, B.; Xin, Y.; Liu, S. Dual-Complementary Convolution Network for Remote-Sensing Image Denoising. *IEEE Geosci. Remote Sens. Lett.* **2021**, *19*, 8018405. [CrossRef]

45. Wang, K.; Chen, H.; Cheng, L.; Xiao, J. Variational-Scale Segmentation for Multispectral Remote-Sensing Images Using Spectral Indices. *Remote Sens.* **2022**, *14*, 326. [CrossRef]
46. Li, J.; Zi, S.; Song, R.; Li, Y.; Hu, Y.; Du, Q. A Stepwise Domain Adaptive Segmentation Network with Covariate Shift Alleviation for Remote Sensing Imagery. *IEEE Trans. Geosci. Remote Sens.* **2022**, *60*, 5618515. [CrossRef]
47. Fuentes, C.M.; Hernández, V. The Spatial Evolution of Employment Subcenters in Ciudad Juárez, Chihuahua (1994–2004): An Analysis Using Global and Local Spatial Autocorrelation Indicators. *Estudios Demográficos Urbanos* **2015**, *30*, 433–467. [CrossRef]
48. Li, Y.; Derudder, B. Dynamics in the Polycentric Development of Chinese Cities, 2001–2016. *Urban Geogr.* **2020**, *43*, 272–292. [CrossRef]
49. Caizhi, S.; Qifei, M.; Liangshi, Z. Analysis of Driving Mechanism Based on a GWR Model of Green Efficiency of Water Resources in China. *Acta Geogr. Sin.* **2020**, *75*, 05001022.
50. Wang, Z.; Fan, C.; Zhao, Q.; Myint, S.W. A Geographically Weighted Regression Approach to Understanding Urbanization Impacts on Urban Warming and Cooling: A Case Study of Las Vegas. *Remote Sens.* **2020**, *12*, 222. [CrossRef]
51. He, X.; Zhang, Z.; Yang, Z. Extraction of Urban Built-up Area Based on the Fusion of Night-Time Light Data and Point of Interest Data. *R. Soc. Open Sci.* **2021**, *8*, 210838. [CrossRef]
52. Cai, J.; Huang, B.; Song, Y. Using Multi-Source Geospatial Big Data to Identify the Structure of Polycentric Cities. *Remote Sens. Environ.* **2017**, *202*, 210–221. [CrossRef]
53. Yang, Z.; Chen, Y.; Guo, G.; Zheng, Z.; Wu, Z. Using Nighttime Light Data to Identify the Structure of Polycentric Cities and Evaluate Urban Centers. *Sci. Total Environ.* **2021**, *780*, 146586. [CrossRef]
54. Strain, E.M.A.; Alexander, K.A.; Kienker, S.; Morris, R.; Jarvis, R.; Coleman, R.; Bollard, B.; Firth, L.B.; Knights, A.M.; Grabowski, J.H.; et al. Urban Blue: A Global Analysis of the Factors Shaping People's Perceptions of the Marine Environment and Ecological Engineering in Harbours. *Sci. Total Environ.* **2019**, *658*, 1293–1305. [CrossRef] [PubMed]
55. Hou, Y. Polycentric Urban Form and Non-work Travel in Singapore: A Focus on Seniors. *Transp. Res. Part D Transp. Environ.* **2019**, *73*, 245–275. [CrossRef]
56. Yang, Z.; Chen, Y.; Wu, Z.; Qian, Q.; Zheng, Z.; Huang, Q. Spatial Heterogeneity of the Thermal Environment Based on the Urban Expansion of Natural Cities Using Open Data in Guangzhou, China. *Ecol. Indic.* **2019**, *104*, 524–534. [CrossRef]
57. Liu, C.; Tang, Q.; Xu, Y.; Wang, C.; Wang, S.; Wang, H.; Li, W.; Cui, H.; Zhang, Q.; Li, Q. High-Spatial-Resolution Nighttime Light Dataset Acquisition Based on Volunteered Passenger Aircraft Remote Sensing. *IEEE Trans. Geosci. Remote Sens.* **2021**, *60*, 1001817. [CrossRef]
58. Li, Y.; Ye, H.; Gao, X.; Sun, D.; Li, Z.; Zhang, N.; Leng, X.; Meng, D.; Zheng, J. Spatiotemporal Patterns of Urbanization in the Three Most Developed Urban Agglomerations in China Based on Continuous Nighttime Light Data (2000–2018). *Remote Sens.* **2021**, *13*, 2245. [CrossRef]
59. Li, X.; Zhao, L.; Li, D.; Xu, H. Mapping Urban Extent Using Luojia 1-01 Nighttime Light Imagery. *Sensors* **2018**, *18*, 3665. [CrossRef]
60. Sun, B.; Zhang, Y.; Zhou, Q.; Zhang, X. Effectiveness of Semi-Supervised Learning and Multi-Source Data in Detailed Urban Landuse Mapping with a Few Labeled Samples. *Remote Sens.* **2022**, *14*, 648. [CrossRef]
61. Zikirya, B.; He, X.; Li, M.; Zhou, C. Urban Food Takeaway Vitality: A New Technique to Assess Urban Vitality. *Int. J. Environ. Res. Public Health* **2021**, *18*, 3578. [CrossRef]
62. You, H.; Jin, C.; Sun, W. Spatiotemporal Evolution of Population in Northeast China during 2012–2017: A Nighttime Light Approach. *Complexity* **2020**, *2020*, 3646145. [CrossRef]
63. Wang, X. Research on the Development Model of Chinese Urban and Rural Big Data Integration Brand Project Based on Ecological Perspective. *J. Phys. Conf. Ser.* **2021**, *1992*, 022124. [CrossRef]
64. Ma, S.; Cai, Y.; Ai, B.; Xie, D.; Zhao, Y. Delimiting the Urban Growth Boundary for Sustainable Development with a Pareto Front Degradation Searching Strategy Based Optimization Model. *J. Clean. Prod.* **2022**, *345*, 131191. [CrossRef]
65. Su, Y.; Wang, Y.; Wang, C.; Zhou, D.; Zhou, N.; Feng, W.; Ji, H. Coupling Relationships between Urban Form and Performance of Outdoor Environment at the Pedestrian Level. *Build. Environ.* **2022**, *213*, 108514. [CrossRef]
66. Ma, M.; Lang, Q.; Yang, H.; Shi, K.; Ge, W. Identification of Polycentric Cities in China Based on NPP-VIIRS Nighttime Light Data. *Remote Sens.* **2020**, *12*, 3248. [CrossRef]
67. He, X.; Cao, Y.; Zhou, C. Evaluation of Polycentric Spatial Structure in the Urban Agglomeration of the Pearl River Delta (PRD) Based on Multi-Source Big Data Fusion. *Remote Sens.* **2021**, *13*, 3639. [CrossRef]
68. He, J.; Li, X.; Liu, P.; Wu, X.; Zhang, J.; Zhang, D.; Liu, X.; Yao, Y. Accurate Estimation of the Proportion of Mixed Land Use at the Street-Block Level by Integrating High Spatial Resolution Images and Geospatial Big Data. *IEEE Trans. Geosci. Remote Sens.* **2020**, *59*, 6357–6370. [CrossRef]
69. Im, J.; Lu, Z.; Rhee, J.; Jensen, J.R. Fusion of Feature Selection and Optimized Immune Networks for Hyperspectral Image Classification of Urban Landscapes. *Geocarto Int.* **2012**, *27*, 373–393. [CrossRef]
70. Cao, R.; Tu, W.; Yang, C.; Li, Q.; Liu, J.; Zhu, J.; Zhang, Q.; Li, Q.; Qiu, G. Deep Learning-Based Remote and Social Sensing Data Fusion for Urban Region Function Recognition. *ISPRS J. Photogramm. Remote Sens.* **2020**, *163*, 82–97. [CrossRef]
71. Ma, X.; Li, C.; Tong, X.; Liu, S. A New Fusion Approach for Extracting Urban Built-up Areas from Multisource Remotely Sensed Data. *Remote Sens.* **2019**, *11*, 2516. [CrossRef]
72. Zhong, Y.; Cao, Q.; Zhao, J.; Ma, A.; Zhao, B.; Zhang, L. Optimal Decision Fusion for Urban Land-Use/Land-Cover Classification Based on Adaptive Differential Evolution Using Hyperspectral and LiDAR Data. *Remote Sens.* **2017**, *9*, 868. [CrossRef]

73. Ma, X.; Tong, X.; Liu, S.; Luo, X.; Xie, H.; Li, C. Optimized Sample Selection in SVM Classification by Combining with DMSP-OLS, Landsat NDVI and GlobeLand30 Products for Extracting Urban Built-Up Areas. *Remote Sens.* **2017**, *9*, 236. [CrossRef]
74. Binter, A.-C.; Bernard, J.Y.; Mon-Williams, M.; Andiarena, A.; González-Safont, L.; Vafeiadi, M.; Lepeule, J.; Soler-Blasco, R.; Alonso, L.; Kampouri, M.; et al. Urban Environment and Cognitive and Motor Function in Children from Four European Birth Cohorts. *Environ. Int.* **2021**, *158*, 106933. [CrossRef] [PubMed]